Real-time Determination of Porosity Development in Carbons: A Combined SAXS/TGA Approach

J.M. Calo,[1] P.J. Hall,[2] S. Houtmann,[2] D. Lozano Castello,[3] R.E. Winans,[4] S. Seifert[4]
[1]Division of Engineering, Brown University, Providence, RI, U.S.A.
[2]Department of Chemical Engineering, Strathclyde University, Glasgow, Scotland, United Kingdom
[3]Departamento de Química Inorgánica, Universidad de Alicante, Alicante, Spain
[4]Chemistry Division, Argonne National Laboratory (ANL), Argonne, IL, U.S.A.

Introduction

Small-angle scattering (SAS) techniques offer a number of advantages for investigating the nature and behavior of porous materials. With respect to carbons in particular, the nonintrusive nature of SAS means that, in principle, characterization can be performed on carbons *in situ* during activation processes, allowing real-time resolution of porosity development. These types of studies were not practical or possible heretofore, primarily because of the prohibitively long counting times required to span the requisite wave vector (q) range over the entire burnoff process. However, the availability of new instruments, such as the small-angle x-ray scattering (SAXS) facility at the APS, has now made these types of experiments possible.

Some preliminary data from these efforts were reported on previously [1]. Here we present results incorporating a thermogravimetric analyzer in the beamline to directly correlate burnoff with SAXS data. Results on the behavior of some different carbons during activation in oxygen are presented, as well as the effect of a catalytic agent, calcium.

Methods and Materials

The SAXS instrument was constructed at ANL and used on BESSRC undulator beamline ID-12 at the APS. Monochromatic x-rays (8.98 keV) were scattered off the samples and collected on a 15 × 15-cm Mosaic charge-coupled device (CCD) array (1538 × 1538 pixels). This system is capable of a resolution of ~0.5 second. The scattered intensities were corrected for absorption, empty cell scattering, and instrument background.

A Cahn TG-121 thermogravimetric apparatus (TGA) was adapted for use directly in the beamline. Two holes, approximately 2 cm in diameter and located 180° apart, were drilled through the walls of the TGA furnace to accommodate the x-ray beam. Two corresponding holes were also made in the quartz hangdown tube of the TGA to admit the x-ray beam. Char samples on the order of tens of milligrams, contained in aluminum foil packets with multiple perforations (to allow for adequate transport of oxygen through the sample), were suspended from the microbalance on a platinum wire.

The experimental arrangement and procedures were gradually improved as experience with the system increased. Since the TGA system was operated in an "open" mode, the reaction gas (oxygen) was used to purge the quartz hangdown tube to maintain uniform composition and temperature. With the flow rate set too high, the sample tended to oscillate on the platinum wire. This resulted in some observable oscillation in scattering intensity at high time resolutions. This problem was solved by lowering the oxygen flow rate to the point where sample oscillation vanished. Also, the location of the sample thermocouple, necessitated by the experimental arrangement, resulted in a systematic offset in the temperature measurements. This problem was rectified via calibrations of the sample temperature in a laboratory TGA.

Samples of saran and microgranular cellulose that weighed 10 g were obtained from the Aldrich Chemical Co. They were heated in a tube furnace at 10K per minute (10K/min) to 900°C, with a 1-hour heat soak time, under flowing nitrogen. Calcium-loaded cellulose was prepared by mixing with calcium acetate solution, followed by drying. The resultant calcium content was approximately 3% following carbonization.

Results and Discussion

Saran Char

The TGA data presented in Fig. 1 were obtained under nonisothermal conditions in an atmosphere of oxygen. As shown, the sample was first rapidly heated to 200°C, held at that temperature for 2 minutes, and then heated to 560°C at 6 K/min, followed by an isothermal period at the final temperature. The bulk of the sample burnt out at about 52 min, before the final temperature was attained. From this point on, the mass signal appeared to be due to the slow burnout of residual and presumably more unreactive material.

SAXS scattering curves corresponding to selected points during the activation history are presented in Fig. 2. In the absence of other effects, scattering at high q values was primarily due to small microporosity, while scattering at low values was due to meso- and larger

porosity [2]. The plateau at high q was indicative of a significant population of micropores. At low burnoffs, there was a notable decrease in the mesoporosity, accompanied by microporosity development at high q. Thereafter, scattering from the microporosity decreased markedly as carbon is burned off.

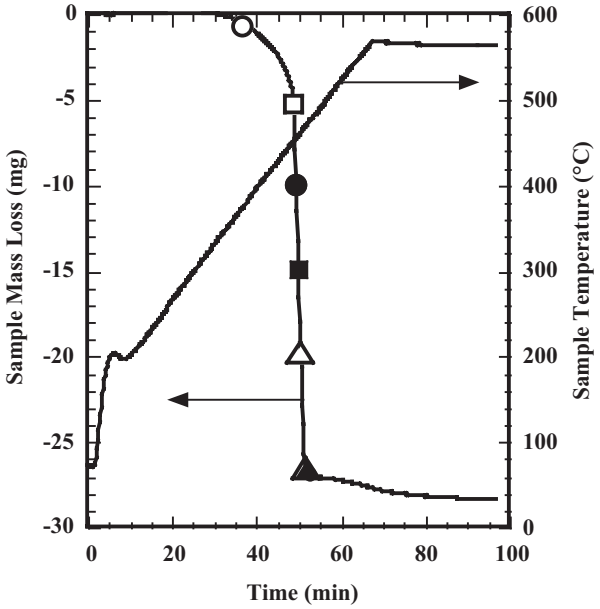

FIG. 1. Saran char sample mass history during nonisothermal activation in oxygen. The symbols correspond to scattering curves in Fig. 2.

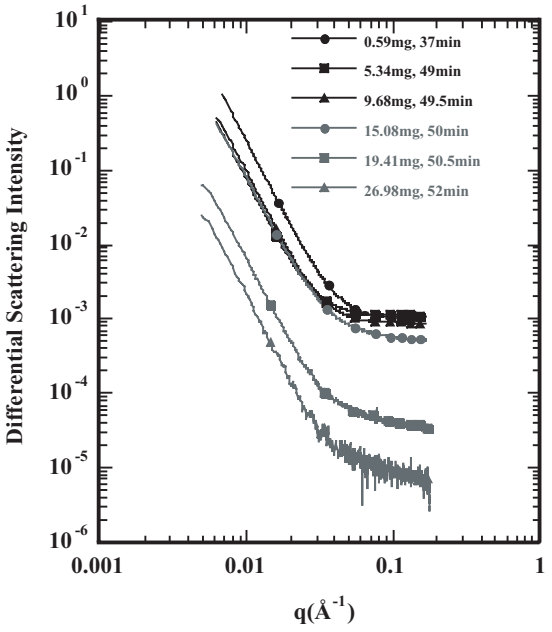

FIG. 2. SAXS curves for saran char during nonisothermal activation in oxygen to 565°C to the indicated mass losses corresponding to the symbols in Fig. 1.

Somewhat similar results were obtained for saran char under near-isothermal conditions in oxygen. The sample temperature was increased at 60K/min to 435°C and then held there. The sample mass actually began to decrease before isothermal conditions were attained. This illustrates the difficulty of resolving the porosity development history under isothermal conditions, where the burnoff behavior typically varies widely depending on the nature and preparation history of the sample. Nonisothermal temperature programs appear to be more efficient in this regard.

The corresponding scattering data are presented in Fig. 3. The variation in scattering intensity with activation appears to be somewhat complex. It is important to note that only *net* porosity differences are observed. Thus, the predominant behavior in the low-burnoff regime (0-7.5 min) appears to be net microporosity development, while scattering from the larger (meso- and larger) pores remains relatively more constant. However, as can be observed from the continuing burnoff history in Fig. 3, the process becomes inverted such that the predominant behavior appears to become net consumption of *mesoporosity,* while the net microporosity remains relatively constant.

The apparent behavior of porosity with activation obtained from raw scattering data is somewhat distorted by the variation of the solid volume fraction ϕ_s in the following manner. The total scattering intensity is given by:

$$I(q) = b_v^2 \, V \, \phi_s(1 - \phi_s) \int_o^\infty \gamma \, [\sin(qr)/qr] \, 4\pi r^2 dr, \qquad (1)$$

where I(q) is the scattering intensity at a value of the scattering wave vector, $q = 4\pi \sin(\theta)/\lambda$, θ is the scattering half-angle, λ is the neutron wavelength, γ is the correlation function, b_v is the contrast factor between solid and voids, and V is the scattering volume. The mean square of the fluctuations of the scattering length density is $b_v^2\phi_s(1 - \phi_s)$, which varies with ϕ_s and thus acts as a scaling factor for the scattering intensity. One way to account for this effect is to correct the scattering intensities with the Porod invariant (PI) [3]:

$$PI = \int_o^\infty q^2 \, I(q) \, dq = 2\pi^2 \, b_v^2 \, V \, \phi_s(1 - \phi_s). \qquad (2)$$

Since all the parameters on the righthand side of this expression should be constant with activation except for ϕ_s, the value of the PI will vary with the behavior of $\phi_s(1 - \phi_s)$. Thus, division of the scattering intensities by this factor can be used to correct for the variation of ϕ_s. It is emphasized, however, that this is only an approximation for a number of reasons, including the fact that when I(q) varies with q to an exponent less than –2 (as it does at high q for the current data), the integral

diverges [3], and accurate values of the PI cannot be obtained.

The PIs calculated from the scattering curves presented in Fig. 3 were found to initially increase up to about 10.29 mg mass loss and then decrease monotonically thereafter. The scattering curves in Fig. 3, corrected by the PI, are presented in Fig. 4. The principal effect of the correction is to draw the curves much closer together, especially for the smallest pores. As shown in Fig. 4, the curves all seem to intersect at a q of ≈0.045 $Å^{-1}$. The population of the larger micro- and mesopores at lower q decrease monotonically with activation up to about 29.59 mg mass loss, then increase with activation beyond this point.

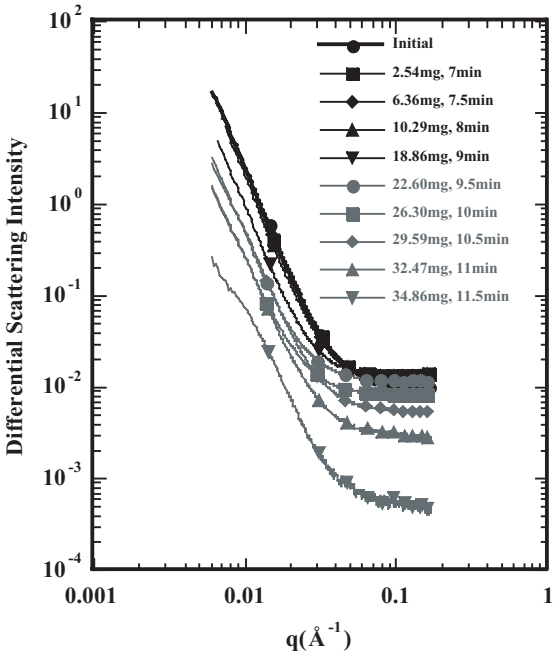

FIG. 3. SAXS curves for saran char activated at 435°C in oxygen to the indicated mass losses.

As shown in Fig. 4, the population of the smaller micropores (q of >0.045 $Å^{-1}$) develops slowly with activation until about 10.29 mg mass loss. It then increases more rapidly to 32.47 mg mass loss, and it decreases thereafter. Note that the decrease in the smallest pores coincides with the point at which the larger pores begin to increase. This behavior is consistent with pore wall collapse among the smallest pores.

These data suggest a dynamic porosity development mechanism beginning with depletion of the larger micro- and mesoporosity and the development of the smaller microporosity. At higher burnoffs, the process changes to one of net loss of the smallest microporosity, while the net population of the larger micro- and mesopores increases. Of course, only *net* porosity differences are observed. Thus, for example, when the porosity in one particular size range is relatively constant, this could occur either because no appreciable reaction occurs in those pores at that particular stage in the activation or because the rates of consumption and development are in relative balance over this burnoff range. Since it would be difficult to reconcile the former mechanism with the nature of the activation process, it appears that the net population balance of pores in a particular size range is responsible for these observations.

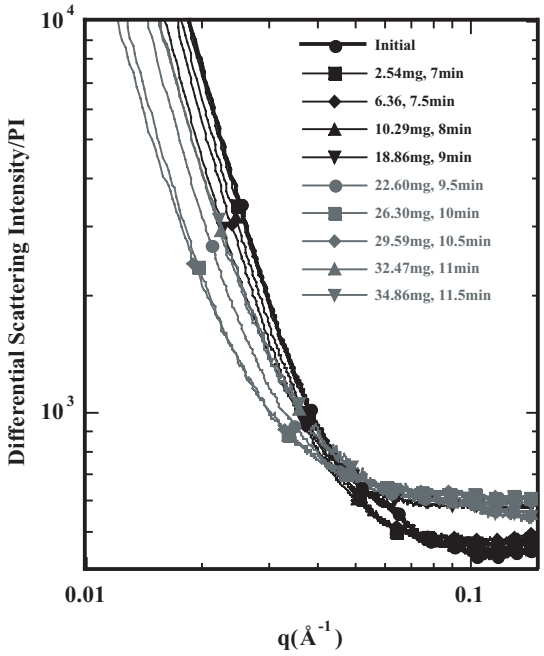

FIG. 4. SAXS curves for saran char from Fig. 3), corrected by the corresponding PIs.

Cellulose Char

Scattering data for a cellulose char sample activated isothermally at 425°C, corrected by the PI values, are presented in Fig. 5. These data show that this carbon, like the saran char, initially exhibits a significant amount of microporosity, as indicated by the plateau centered at about q = 0.1 $Å^{-1}$. The PIs for these data initially increase and then decrease with activation, as occurs in the saran char case. However, there are some differences as well. As shown in Fig. 5, initially the population of the smallest micropores centered at about 0.1 $Å^{-1}$ increases much more markedly than it does in the saran char case. This is accompanied by relatively little development of the larger porosity, following a significant initial loss at low q values. However, continued net microporosity development with activation then slows significantly and finally begins to decrease, while the population of the larger pores increases rapidly. Once again, just as in the

saran char case, this change in behavior coincides with a decreasing population of the smallest pores, consistent with pore wall collapse among the smallest pores.

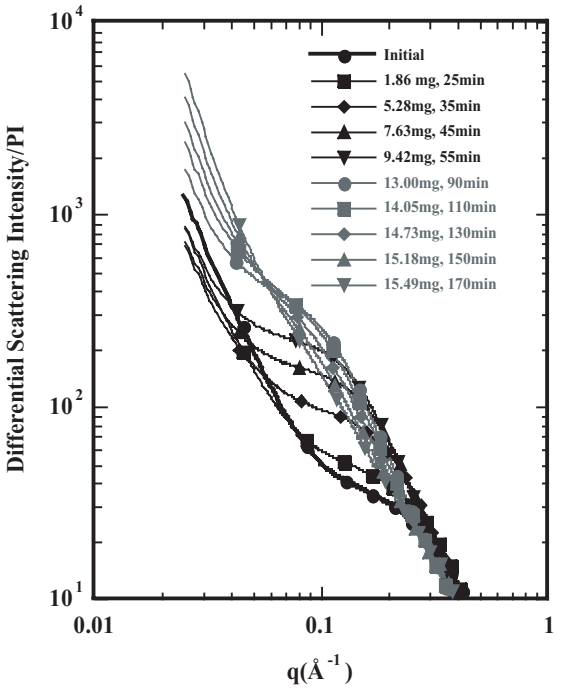

FIG. 5. SAXS curves for cellulose char activated at 425°C in oxygen to the indicated mass losses, corrected for the corresponding PIs.

Differences in the behavior of the microporosity in the saran and cellulose chars may be related to "closed porosity." It is well known that "glassy" carbons can exhibit a considerable amount of microporosity that is initially "blocked" from access to the activating agent by more reactive, less ordered carbon. Early activation of these types of carbons primarily involves preferential burnoff of this carbon, exposing the intrinsic underlying microporous structure. For example, when contrast-matching small-angle neutron scattering (SANS) was used, no new microporosity development was observed upon activation of a char produced from a highly cross-linked phenol-formaldehyde resin up to 21% burnoff [2]. The only mechanism observed was unblocking of initially "closed" microporosity. Unfortunately, SAXS is not amenable to contrast matching as is SANS. Consequently, this approach could not be used in the current experiments. However, a similar mechanism may be at least partially responsible for the relatively slower and less marked evolution of microporosity with activation in the saran char than in the cellulose char.

Calcium-loaded Cellulose Char

Mass loss data for the Ca-loaded char are unavailable since these data were obtained prior to the TGA being incorporated into the experimental system. A 1-mm-diameter quartz capillary was used as the sample holder. The scattering data for this sample, corrected by the PI values, are presented in Fig. 6. The PIs for these data increase monotonically with activation. No maximum was observed as it was for the saran char and unpromoted cellulose char samples. As shown, the behavior of the Ca-loaded cellulose char differs significantly from that of the unpromoted cellulose (compare with Fig. 5). Initially, the scattering intensity remains relatively constant and actually decreases lightly with activation over the entire q range. This behavior is similar to that observed for phenolic resin char at low q at low burnoffs, which was attributed primarily to the preferential gasification of disordered carbon clusters having characteristically large sizes [2]. This is followed by a pattern of rapidly increasing scattering intensity at lower q values (q of <0.045 Å^{-1}) than those for the unpromoted cellulose char, which continues to progressively shift to lower q with activation. As shown, there appears to be little small microporosity development (q of >0.045 Å^{-1}) over the entire activation history. The preferential development of mesoporosity rather than microporosity in the Ca-loaded char may be due to the catalytic effect of calcium, which may not have been well-dispersed in the smallest pores.

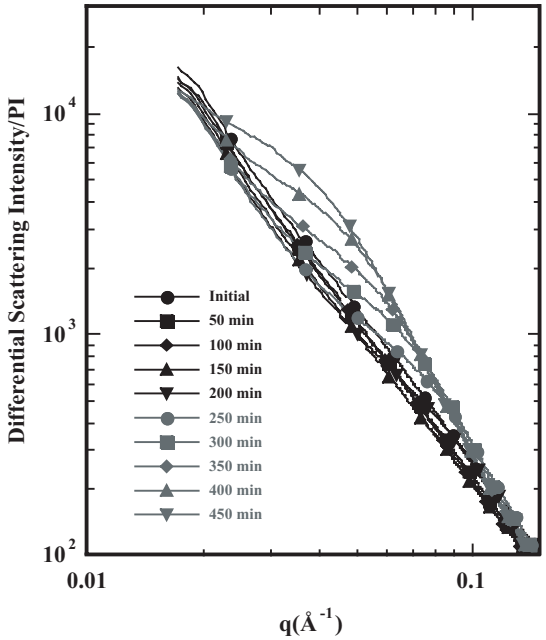

FIG. 6. SAXS curves for Ca-loaded cellulose char during isothermal activation at 340°C in oxygen, corrected by the corresponding PIs.

Acknowledgments

The authors acknowledge support from the Engineering and Physical Sciences Research Council (EPSRC) under Grant No. GR/N03006. Use of the APS was supported by the U.S. Department of Energy, Office of Science, Office of Basic Energy Sciences, under Contract No. W-31-109-ENG-38.

References

[1] J.M. Calo, P.J. Hall, S.D. Brown, R.E. Winans, and S. Seifert, in *Eurocarbon 2000*, Proceedings of the First World Conference on Carbon (Berlin, Germany, 2000), pp. 113-114.

[2] M.M. Antxustegi, P.J. Hall, and J.M. Calo, J. Colloid Interface Sci. **202**, 490-498 (1998).

[3] J.S. Higgins and H.C. Benoît, *Polymers and Neutron Scattering* (Oxford University Press, Oxford, England, 1994).